ELSEVIER

Polymer 42 (2001) 8975–8985

polymer

www.elsevier.com/locate/polymer

Structure and morphology of PET/PEN blends

Terry D. Patcheak, Saleh A. Jabarin*

Polymer Institute, University of Toledo, Toledo, OH 43606-3390, USA

Received 26 February 2001; received in revised form 30 March 2001; accepted 30 March 2001

Abstract

Blends of poly(ethylene terephthalate) (PET) and poly(ethylene naphthalate) (PEN) have been analyzed in terms of their crystal structures and morphologies. Wide angle X-ray diffraction (WAXS), small angle X-ray diffraction (SAXS), and density measurements were performed on blend samples crystallized quiescently and on samples strain induced crystallized. For blends quiescently crystallized isothermally, the crystallite dimensions calculated from the WAXS diffraction patterns via the Scherrer equation, along with the results from the SAXS, led to the conclusion that the blends crystallized independently. This means the major component of the blend crystallized, while the minor component did not crystallize and was forced into the interlamellar amorphous region. WAXS studies on the strain induced crystallized samples showed a change in the lattice parameters with composition, leading to the conclusion of co-crystallization for these blends. Density measurement showed a decrease in density with increasing PEN content indicating a reduction of the percent crystallinity of the blends as compared to the unblended homopolymers.

Keywords: PET/PEN block copolymers; Copolyesters; X-ray diffraction

1. Introduction

Poly(ethylene terephthalate) (PET)/poly(ethylene naphthalate) (PEN) blends and copolymers are of commercial interest due to their thermal, mechanical and barrier properties. As a result, their properties have become of the focus of many articles [1–12]; however, little has been reported on their structures and morphologies, which are the controlling factors for their physical properties. In this work, the structures and morphologies of a series of PET/PEN blends have been investigated using wide-angle X-ray diffraction (WAXS), small angle X-ray diffraction (SAXS), and density. The effects of strain-induced crystallization versus isothermal quiescent crystallization have also been examined.

When PET and PEN are melt blended together, the end groups react with each other through a reaction called transesterification. This reaction creates PET/PEN block copolymers that act as a compatibilizer between the PET and PEN phases, improving miscibility [13–19] of the blends. This is important for the creation of optically clear products. Many factors have been found to affect the transesterification reaction kinetics including blending time, melt temperature, catalyst system, and composition [19,20]. It has also been found [20] that the viscosity ratio of the two homopolymers making up the blend, play an important role in the transesterification kinetics. Finally, the reaction kinetics can be modified by capping the hydroxyl end groups of the PET and PEN homopolymers [21].

As mentioned before, transesterification creates PET/PEN block copolymers thus improving miscibility. As the extent of this reaction increases, two things occur. First, more block copolymers are formed, further improving miscibility; and second, the PET and PEN sequence lengths of the existing PET/PEN block copolymers decrease making the copolymer more random in nature. The level of transesterification is measured through the polymer's degree of randomness (DR). The level of the DR is important because it affects the properties of the resultant blends [22,24–30]. At 100% reaction level (DR = 1), a blend becomes equivalent to a statistical random copolymer as synthesized by melt polymerization.

Previous work [12,30] has shown that the properties of a PET/PEN blend, below a given DR, vary with both the DR and the composition of the blend. Past some critical level of DR the blend's properties become constant with the DR, and vary only with the composition of the blend. This is significant because in industrial applications, blends processed through extrusion or injection molding will have experienced varying amounts of transesterification from one batch to another. As a result, the properties of the resultant

* Corresponding author. Tel.: +1-419-530-5005; fax: +1-419-530-5019.
E-mail address: sjabari@utnet.utoledo.edu (S.A. Jabarin).

0032-3861/01/$ - see front matter
PII: S0032-3861(01)00383-4

blends could vary. This however can be avoided, as long as the blends have been transesterified past their critical DR. The processing conditions needed to achieve critical transesterification, as well as the rheological and degradation kinetics of PET/PEN blends have been studied by Tharmapuram and Jabarin [31,32].

PET and PEN are both crystallizable polymers. PET has only an α crystal form, which is triclinic [33–35]. PEN has two crystal forms, α and β, which are both triclinic [36–38], and have been found to be dependent on the temperature of crystallization [10,36,39]. Buchner, Wiswe, and Zachmann [36] report that when it is crystallized below 200°C, only the α form of PEN is obtained. When crystallization is performed at higher temperatures, the crystal form is dependent on the sample's prior history of melting. If the PEN was melted at 280°C and subsequently crystallized above 200°C, the β form is obtained; however, if melting was performed at temperatures higher than 320°C, then the α form is obtained during subsequent crystallization at equivalent temperatures. Cakmak and Kim [39] found similar effects in the morphology of high-speed spun PEN fibers. They found the PEN remains amorphous at low spinning speeds and crystallizes at higher spinning speeds. In addition, as the take-up speed increases, the percent β phase relative to the α phase of the crystals increases. They attributed this transition to the fact that increasing the take-up speed increases the temperature.

The crystallization kinetics partly determines the morphology of the crystals. Shi and Jabarin studied the crystallization kinetics as well as the melting and glass transition temperatures of PET/PEN blends after critical transesterifification had been achieved [12,40]. Using DSC, they studied the Avrami kinetics of isothermally crystallized samples. It was found [40] that the blends had different Avrami exponents than the pure components. In all cases, Avrami exponents of three or four were obtained indicating a spherulitic superstructure. Using equilibrium melting point data [12], they further described the microcrystalline structure of these systems in a qualitative manor using Flory's theory of crystallizing copolymers [41]. They found the equilibrium melting temperatures exhibited a minimum value with increasing PEN content. Based on this observation they concluded that the major blend component is crystallizing, while the minor component is being forced into the amorphous phase. It should be noted, however, that this is not conclusive proof, and that to fully prove the type of crystal system, X-ray diffraction should be performed.

Flory [41] first described crystallization of copolymers by saying they consist of units of type A, which are crystallizable, and units of type B, which are not crystallizable. Component A was considered to be homopolymer sequences, occurring by chance in the polymer backbone that could segregate out and crystallize. Wunderlich [42] further constrained Flory's model by saying only nearest neighbors could crystallize without sequence redistribution, and that all other units could be considered as defects. More recently, Windle [43] has suggested that the crystal system may come from segregating and lateral matching of similar yet random sequences of neighboring molecules.

There are two types of crystallization systems. First, PET and PEN can crystallize independently of one another. This creates separate crystalline regions for both PET and PEN. This is termed independent crystallization. In an X-ray analysis, the data would show diffraction peaks of the crystallizing component without any peak shifting. The other type of crystal systems is a mixed crystal system, which is called co-crystallization. Co-crystallization occurs when one component replaces the other in the crystalline regions. Here, the crystalline regions would contain both PET and PEN. This type of crystallization system would exhibit crystalline diffraction peaks of the major component; however, they would be shifted slightly since the crystal lattice would be distorted.

Lu and Windle [44,45] used X-ray diffraction to study the compositional effects on annealed strain induced crystallized fibers of PET/PEN copolymers. In their studies, the copolymers were made through melt polymerization and not blending; therefore, their samples' DR were equal to one. They examined the long period and the projected unit cell dimensions and found that the reciprocal lattice coordinates shifted smoothly from that of pure PET to that of pure PEN. This distortion of the reciprocal lattice coordinates led to the conclusion that the copolymers co-crystallize. They also studied the long period of the fibers and found it to be around 12.0 and 14.5 nm for pure PET and PEN, respectively. For the intermediate compositions, it reached a maximum of around 22.5 nm for the 50% PEN composition.

Jun et al. [46] studied the relationship between block length and the material's ability to crystallize for PET/PEN copolymers and blends. Their blends were highly transesterified and contained a high degree of randomness. These values ranged from 0.692 to 1.0, which is the value for the statistical random copolymer. Because these values are so high, the blends were essentially copolyesters with very small block lengths. Using DSC measurements, they found that there is a critical block length below which PET/PEN systems do not crystallize. This critical block length was three. If the samples' major component had a block length over three, they found it would crystallize independently. They confirmed this with WAXS. Similar results have been found for poly(butylene succinate)/poly(butylene terephthalate) blends [47].

Wu and Cuculo [48] prepared melt-spun fibers of PET/PEN blends at various take-up speeds. At low to moderate take-up speeds, only PEN was found to give a crystalline WAXS profile. The amorphous natures of the PET/PEN samples were also verified using DSC. These samples were then annealed above their cold crystallization temperatures and evaluated. Based on the WAXS profiles, it was concluded that independent crystallization of the major component had occurred. Although these results are

Table 1
Degree of randomness and block lengths for PET/PEN blends

Blend composition (wt%)	DR	Block length PET	Block length PEN
5% PEN	0.113	164	9
20% PEN	0.115	41	7
40% PEN	0.106	22	16
60% PEN	0.211	8	12
80% PEN	0.296	4	63

different from those reported by Lu and Windle, who observed co-crystallization of fibers, the differences originate from the variation in the preparation techniques of the samples. Wu and Cuculo annealed fibers that had been wound-up at low take-up speeds. No crystalline diffraction peaks were seen in these samples before annealing, except for that of PEN; therefore they appeared to be substantially amorphous in nature. When these samples were annealed above their cold crystallization temperatures, they most likely underwent thermal crystallization, which led to independent crystallization of the major component.

As was discussed, PET/PEN systems have been widely studied; however, most work has been directed at their properties. Fewer investigations have been focused on the structures and morphologies of these systems, which are the controlling factors for their physical properties. The structures of strain induced crystallized random PET/PEN copolyesters have been examined. PET/PEN blends, however, have much larger block lengths than their corresponding copolyesters, and their structures and morphologies have only recently begun to be investigated. The objective of this work is to present a detailed analysis of the structures and morphologies for PET/PEN blends that have been transesterified past their critical DR. The effects of quiescent versus strain induced crystallization modes will also be elucidated.

2. Experimental

2.1. Blending of PET/PEN blends

The PET homopolymer used in this study was provided by Eastman Chemical and had an intrinsic viscosity of 0.72. This was measured in a phenol/tetrachloroethane solution at 25°C. It was used for both the pure PET samples and in the PET/PEN blends. The PEN homopolymer used for the blends was provided by Hoechst Celanese and had an intrinsic viscosity of 0.57. This was measured in phenol/tetrachloroethane at 30°C. PEN from BP Amoco Chemicals, with an intrinsic viscosity of 0.62, was used for the pure PEN samples.

The materials were vacuum dried at 120°C for 20 h and then melt-blended at 300°C using a single screw extruder [20,30]. The resultant blend ribbons were cut up, re-dried, and then similarly melt blended in the extruder for a second and third time. This was done to ensure the blends had surpassed their critical level of transesterification, which was measured using proton nuclear magnetic resonance [20,30]. These values are reported in Table 1 along with their corresponding PET and PEN block lengths. These were calculated using equations one and two [7].

$$L_T = 1/(1 - X_T)\mathrm{DR} \quad (1)$$

$$L_N = 1/(1 - X_N)\mathrm{DR} \quad (2)$$

where L_T is the average sequence lengths of ethylene terephthalate units, L_N, the average sequence lengths of ethylene naphthalate units, X_T, X_N, the molar fraction, and DR is the degree of randomness.

3. Measurements

3.1. Wide angle X-ray diffraction

WAXS measurements were performed using a Scintag XDS2000 diffractometer with a copper radiation source (0.15406 nm) and solid state germanium detector cooled by liquid nitrogen. The power settings for the X-ray source were 45 kV and 40 mA. Divergent beam slits of 2 and 4 mm were used after the X-ray source. Convergent receiving slits of 1 and 0.3 mm were used before the detector. Scans were made over the two theta range 10–60° at 1°/min using a step size of 0.03°. Measurements were taken at room temperature, in air and at normal pressure. The software used to process the data was DMS2000 version 3.43 on MicroVAX 3100. K-β radiation was found to be negligible in intensity and therefore no correction was made. All films studied were quiescently crystallized using a Mettler hot stage and FP-82 control unit after being dried at 60°C for at least two weeks. For these samples and all others prepared in this study, crystallization was performed isothermally. Crystallization times were at least ten times the half time of crystallization as determined by differential scanning calorimetry (DSC)[30,40].

In order to study the effects of the modes of crystallization, strain induced crystallized samples were made using an Instron with a heated chamber. Stretching was performed uniaxially unconstrained at a rate of 50 in./min at a temperature of 30°C above the respective glass transition temperatures of each blend. A stretch ratio of four times, or 300%, was achieved.

3.2. Density

Samples for density measurements were prepared by first drying the sample for two weeks at 60°C. The samples were then quiescently crystallized for at least 10 times their half times of crystallization as determined by DSC [30,40]. After crystallization, samples were stored in a constant temperature, constant humidity room. This was done to ensure all

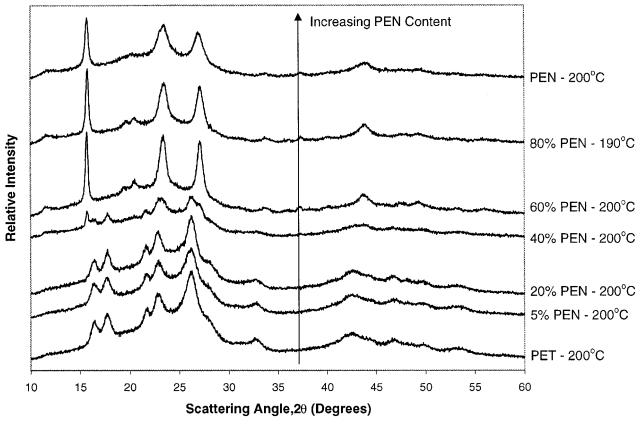

Fig. 1. WAXS profiles for quiescently crystallized PET/PEN blends.

samples had the same preconditions before measurement. Density measurements were then carried out using a density gradient column containing calcium nitrate solution. Glass beads with known densities were placed in the column. A linear interpolation between the two nearest beads was used to determine the sample's density.

3.3. Small angle X-ray diffraction

SAXS experimental data were provided by AMIA laboratories of Austin, TX. The samples were the same as those made for the WAXS experiment. Chromium radiation of 0.22897 nm was used for the X-ray source. A linear background subtraction was performed on the raw data.

4. Results and discussion

4.1. WAXS: quiescently crystallized blends

Fig. 1 shows the relative intensities of the WAXS patterns for the samples quiescently crystallized at various compositions. The scattering pattern of pure PET is at the bottom, and that of pure PEN is at the top. Both the 5 and 20% PEN blends have PET-like diffraction profiles. Similarly, the 60 and 80% PEN blends show α form PEN-like diffraction profiles. In this work, no β form for PEN or for the PEN rich blends was encountered. This is in agreement with work of Zachmann [36]. They found that the crystal form for PEN is dependant on the prior melting temperature. They obtained the β form for PEN crystallized above 200°C when it was previously melted at 280°C, and the α form when it was previously melted at 320°C. At some intermediate temperature, there must be a transition point. In the work for this paper, the blends were previously melted at 300°C. Therefore, the transition temperature from α to β form is likely below 300°C.

If co-crystallization occurs in the blends, then there will be a shifting in the peak positions as the percent PEN is increased. This is due to the PEN distorting the crystal lattice as discussed earlier. No shifting in peak positions was seen for any blends quiescently crystallized. As a result, the 5 and 20% PEN blends indicate that only PET is crystallizing in these blends and that the PEN portion resides in the amorphous phase. Likewise, the 60 and 80% PEN blends show independent crystallization of PEN, with PET being trapped in the amorphous phase.

The 40% PEN blend shows a combined diffraction pattern of PET and PEN superimposed. This is seen more easily in Fig. 2, which shows the 40% PEN blends' diffraction profiles at various crystallization temperatures. At low crystallization temperatures, diffraction patterns similar to that of PET are found. As the crystallization temperature increases, PEN's diffraction profile becomes visible and eventually becomes more distinct than that of PET. The superposition of the two diffraction profiles suggests there are two crystalline phases, a PET rich phase and a PEN rich phase. Neither of the two phases shows any peak shifts; therefore, both phases are crystallizing independently. Furthermore, the amount of one crystalline phase relative to the other crystalline phase is dependent on the temperature of crystallization. This is due to the crystal growth kinetics for both PET and PEN. Generally, each of these materials will crystallize most rapidly midway between the glass transition temperature and the equilibrium melting temperature. This indicates PET's fastest crystallization temperature is near 180°C and that of PEN is near 220°C. The crystallization of pure PEN below 150°C is expected to be very slow, thus requiring the blends be held at these crystallization temperatures for a much longer time to see any crystallization of the PEN. At higher temperatures, PEN crystallizes more readily than PET. Therefore, the pattern becomes more PEN dominant as the crystallization temperature is increased.

In view of the semicrystalline nature of the PET, PEN and PET/PEN blends, the amorphous contributions to the WAXS scattering needs to be removed in order to deconvolute the resulting crystalline peaks. For some isolated peaks, it has been suggested that a linear interpolation can be used to determine the amorphous scattering [49]. This works well

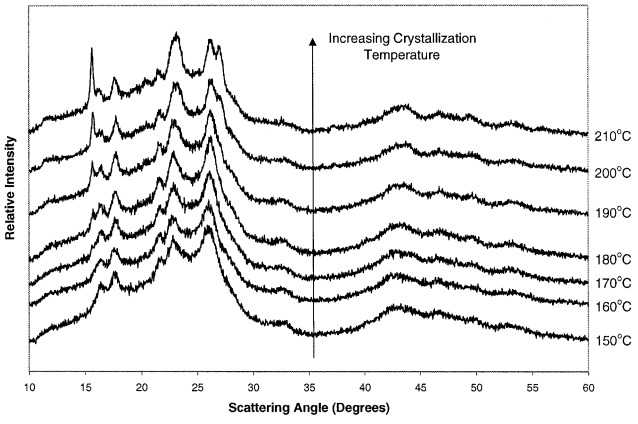

Fig. 2. WAXS profiles for the 40% PEN Blend quiescently crystallized at isothermal temperatures from 150–210°C.

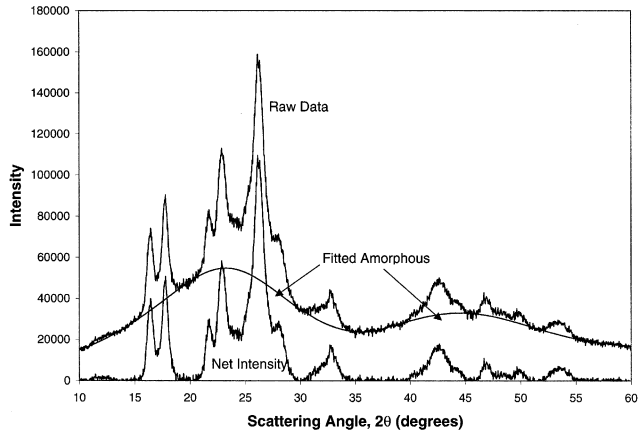

Fig. 3. Typical WAXS raw data before and after amorphous background removal.

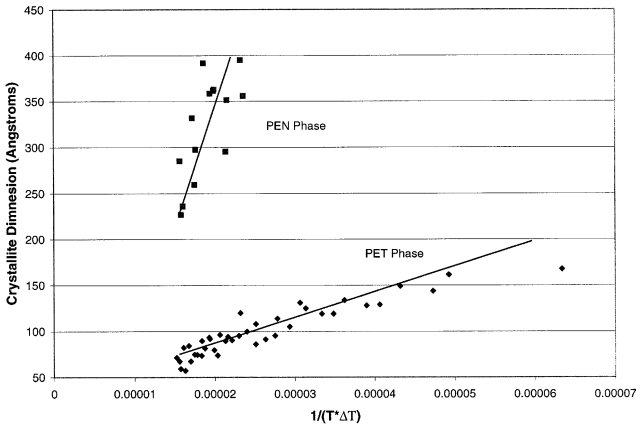

Fig. 4. Degree of supercooling effects on crystallite dimensions for the 010 plane.

for the peaks below 20°, however, the region between 20 and 30° degrees does not contain isolated peaks or a linear background. As a result, this area must be curve fitted as a whole for background removal. Chung and Scott suggest that this amorphous scattering is Gaussian in nature and should be curve fitted as such [50]. In this work, curve fitting was performed on various groupings of data points for each sample. In these fittings, three types of functions were used: linear, Gaussian, and pseudo-Voigt. These are listed in Eqs. (3)–(5), respectively.

Linear

$$y = ax + b \tag{3}$$

Gaussian

$$y = a\exp\left[-0.5\left(\frac{|x - x_0|}{b}\right)^c\right] \tag{4}$$

Pseudo-Voigt

$$y = y_0 + a\left[c\left(\frac{1}{1 + \left(\frac{x - x_0}{b}\right)^2}\right)\right] + (1 - c)\exp\left[-0.5\left(\frac{|x - x_0|}{b}\right)^2\right] \tag{5}$$

where y is the predicted intensity, a, b, c, y_0, x_0 the fitted parameters, and x is the scattering angle.

Typically, the linear function was used for scattering angles less than 20°, while the other two functions were used for scattering angles above 20°.

Fig. 3 shows a typical background subtraction for one of the samples. Once subtracted, the peaks were de-convoluted using the powder SCINTAG software deconvolution program. In the settings, the ratio of $k_{\alpha 1}$ to $k_{\alpha 2}$ radiation was set to a constant. The program then subtracted out the $k_{\alpha 2}$ radiation effects during the deconvolution. Determination of the peaks was based on a Pearson VII distribution. Crystallite dimensions were calculated using the Scherrer equation [51] shown in Eq. (6)

$$L_{hkl} = K\lambda/\beta_0 \cos(\theta) \tag{6}$$

where L_{hkl} is the crystallite dimension perpendicular to plane hkl, hkl the Miller indices K the constant commonly assigned 1, λ, the wavelength of Light, β_0, the integral breadth or breadth at half-maximum intensity, and θ is the scattering angle.

In this equation, the constant (K) was assigned a value of one for all samples.

The true driving force for crystallization is not the crystallization temperature, but rather the degree of supercooling. This is the equilibrium melting temperature minus the crystallization temperature. According to crystal growth theory, Figs. 4–5 show the crystallite dimension as a function of the degree of supercooling as is traditionally reported. Two distinct lines are formed and it becomes apparent that the crystallite dimensions do not change with composition. One line represents the PET crystalline phase and the other line represents the PEN crystalline phase, further proving that the blend components crystallize

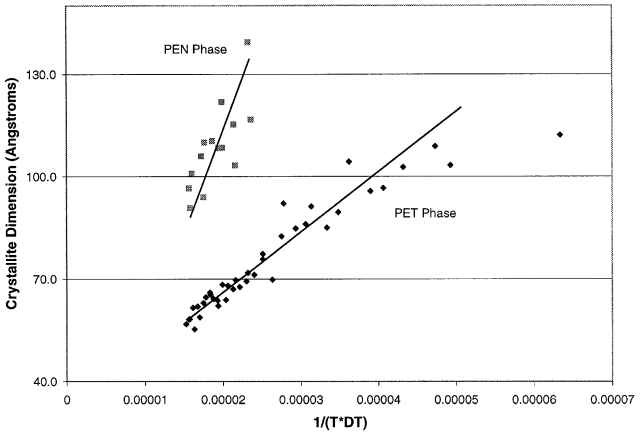

Fig. 5. Degree of supercooling effects on crystallite dimensions for the 100 plane.

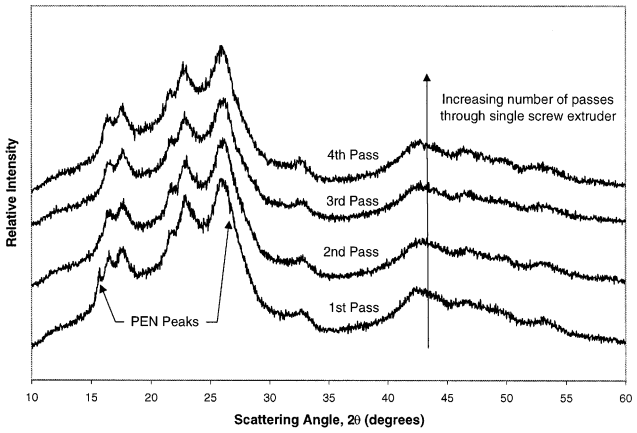

Fig. 6. Effect of number of single screw extruder passes on WAXS profiles obtained for quiescently crystallized 20% PEN blends.

independently. The slopes of the lines are related to the fold and surface free energies. Since the free energies for PET and PEN are different from one another, the slopes of the two lines are different. Slight deviation from linearity is seen at high crystallization temperatures for the 20% PEN blend.

Fig. 6 shows the WAXS patterns for the 20% PEN blends with increasing number of passes through the single screw extruder. In the first two passes there is evidence of both PET and PEN crystallizing. This is to be expected since the first and second passes are mainly physical blends with little transesterification, as shown by the low DR listed in Table 2. By the third pass, the PEN peaks are disappearing, and at the fourth pass the PEN peaks are no longer visible. This is in agreement with results presented in literature [30,40,46]. As discussed earlier, the properties of the blends become constant past a critical DR [30,40]. This critical level is related to when the PEN no longer crystallizes. If two components are crystallizing in a blend, it is not definite that the relative ratios will be the same each time a sample is crystallized. Since the properties of the blend are highly dependent on the level of crystallinity and on the crystallization history, they will be different from one sample to another. If there is a more homogeneous mixture with only one component crystallizing, properties will be relatively constant from sample to sample. This is in agreement with Im et al. [46]. They found that there is a minimum block length needed for the components to crystallize. The increased mixing of the fourth pass through the extruder has then allowed the 20% PEN blends to decrease past this minimum block length. From Tables 1 and 2, the critical block length appears to be around 11. This is different from Im's et al. value of three. This is because different homopolymers were used in each study for the making of the blends. Also, Im et al.'s critical block length was determined using DSC and not WAXS. DSC is more sensitive to crystallization of the minor component than WAXS. This is because the WAXS pattern for a major component could easily mask the minor component's pattern. As a result, the critical block length would be higher for WAXS results. Despite this, there is a critical block length, below which, the minor component does not crystallize.

4.2. WAXS: strain induced crystallization

It is reported that melt polymerized PET/PEN copolymers undergo co-crystallization when strain induced crystallized [44,45]. This has led to the question of whether this was because the statistical random copolymers were used rather than blends, or because the samples were strain induced crystallized rather than quiescently crystallized. In order to clarify these relationships, strain induced crystallized samples were prepared for WAXS analysis. Fig. 7 shows the relative diffraction profiles for the strain induced crystallized samples at various compositions. PET is the lowest curve and PEN is the highest curve. As the percent PEN increases, the pattern changes from that of pure PET to pure PEN. Also, there are definite shifts in the peak positions. This is more clearly seen in Fig. 8, which shows the peak positions at various compositions. The shifting of the d-spacings indicates that the crystal lattice is distorting and that both components are crystallizing. As a result, when PET/PEN blends undergo strain induced crystallization, they co-crystallize.

In summary, Lu and Windle studied copolymers synthesized directly by melt polymerization and found them to co-crystallize when strain induce crystallized. As discussed before, these samples were completely random and had a DR equal to 1. As result, the samples had very short PET and PEN block lengths. In this present study of blends, the DR was closer to 0.1, and therefore samples had larger block lengths. Furthermore, the type of crystallization could be controlled by the method of crystallization. Quiescent isothermal crystallization led to independent crystallization of the major component, while strain induce crystallization led to co-crystallization of both components. This is due to differences in the crystallization kinetics of

Table 2
Degree of randomness and block lengths for 20% PEN blends

Single screw extruder pass	DR	Block length PET	Block length PEN
1st pass	0.005	935	254
2nd pass	0.061	77	21
3rd pass	0.115	41	11
4th pass	0.167	28	7

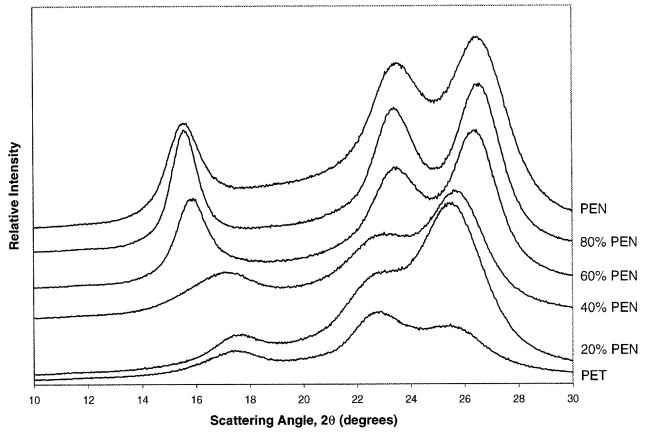

Fig. 7. WAXS profiles obtained for strain induced crystallized PET/PEN blend and homopolymer samples.

the two crystallization methods. When samples are crystallized quiescently, the crystallization process is very slow. The PEN has enough time to reposition itself into the amorphous phase. On the other hand, strain induced crystallization is a very rapid process. All chains, including PEN, are forced into alignment and crystallization occurs simultaneously for both the PET and PEN chains into one phase.

4.3. SAXS

From the WAXS experiments on quiescently crystallized samples, it is known that the major components of the blends crystallize, while the minor components are forced into the amorphous phase. The question remains as to where the amorphous phase containing the minor component resides. There are three possible morphologies [52]. These are dependent on the non-crystallizing component's diffusion coefficient (D) and the velocity of the crystal growth front (G). If D is much greater than G, then the non-crystallizing component will be able to diffuse out of the spherulites altogether. This morphology is termed interspherulitic. If D is much less than G, then the non-crystallizing component will be trapped between the lamella of the spherulite.

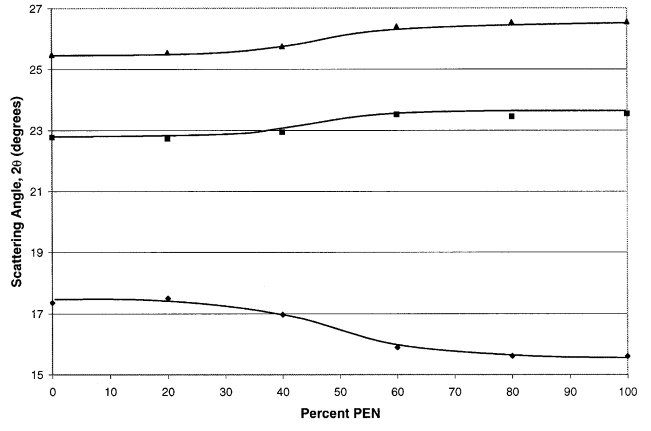

Fig. 8. Changes in peak positions for strain induced crystallized samples.

This morphology is termed interlamellar. The final morphology also occurs when D is less than G and is called interfibrillar or inter(lamellar-bundle). This is when pockets of the non-crystallizing component are trapped within regions of the spherulites. In real systems, all three are most likely present; however, one morphology will generally dominate.

It is assumed that the dominant morphologies for PET, PEN and the blends are interlamellar for several reasons. First, PET and PEN both crystallize in a spherulitic superstructure, which optical microscopy shows to be volume filling, indicating that little if any interspherulitic morphology exists. Second, the benzene and naphthalene rings of the PET and PEN, respectively, stiffen the polymer backbone, thus slowing diffusion. Finally, the transesterification reaction makes it less likely that the minor component could segregate out and form clusters around the spherulites. If interlamellar morphology is dominant, it can be verified using SAXS.

SAXS allows for the calculation of the long period. This is the center-to-center distance of two neighboring lamella. It allows for the calculation of the crystallite size and interlamellar amorphous region size. These are all obtainable using the correlation function shown in Eq. (7) [53–55].

$$\gamma_1(r) = \frac{1}{Q_{\mathrm{SAXS}}} \int_0^\infty \mathbf{q}^2 (I - I_\mathrm{b}) \cos(qr)\, \mathrm{d}q \tag{7}$$

where $Q_{\mathrm{SAXS}} = \int_0^\infty \mathbf{q}^2 (I - I_\mathrm{b})\, \mathrm{d}q$, $\mathbf{q}$ the scattering vector $= (4\pi/\lambda)\sin[\theta]$, I the scattering intensity, I_b the scattering contribution due to scattering from local electron density fluctuations in the amorphous region, and r is the coordinate along which the electron density distribution varies.

In this equation, the intensity must be extrapolated to infinity and to zero. Extrapolation of the intensity to infinity was performed using Porod's law [56]. The Porod constants, K and I_b, were obtained by curve fitting the linear region of a plot of Iq^4 versus $\mathbf{q}^4$. The value of I_b was also used as a correction term for the contribution of intensity due to scattering from local electron density fluctuations in the amorphous region. Extrapolation to zero was performed assuming a linear $[I - I_\mathrm{b}]\mathbf{q}^2$ versus $\mathbf{q}^2$ profile [56]. Fig. 9 shows the correlation function and the parameters obtainable from it. From this plot, the long period can be calculated two ways: twice the position of the first minimum, or from the position of the first maximum. The later was used in this work. Fig. 9 also shows the extrapolation of the characteristic length, l_1. This represents the crystallite height, l_c, or the height of interlamellar amorphous region, la. It is impossible to know which length it really represents, and therefore should be determined through reasoning or through another technique. The corresponding size of the other phase can be simply calculated from the subtraction of l_1 from L.

Fig. 10 shows a typical plot used to determine the Porod constants. A linear regression was used to determine the constants. Little deviation from linearity was seen in the

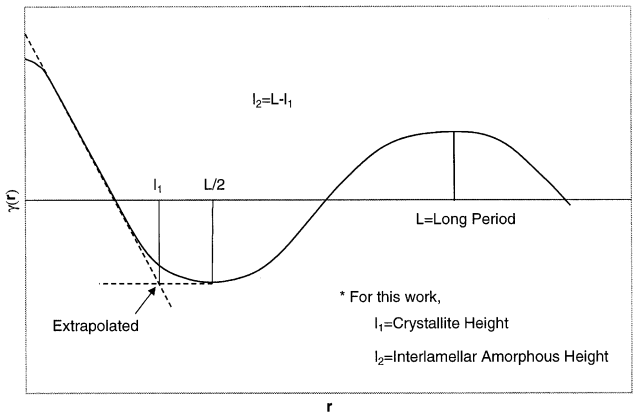

Fig. 9. Example of data obtainable from the correlation function.

samples. Fig. 11 shows the desmeared SAXS curves at various compositions. As the percent PEN increases, the peak position shifts to lower angles. At 60% PEN it reaches a minimum, and then shifts toward higher angles. Since **q** is defined as $4\pi \sin(\theta)/\lambda$, and Bragg's law [57] is $n\lambda = 2d \sin(\theta)$, the peak position is then related inversely to the long period ($L = 2\pi/\mathbf{q}_{max}$). This means the long period shows a maximum value around the 60% PEN composition. Fig. 12 shows the correlation function for the PET/PEN blends. The first maximum increases with percent PEN up to the 60% PEN composition, as was expected from the desmeared plots. The long period derived from the position of the first maximum of the correlation function is plotted in Fig. 13. It is 9.2 and 13.4 for the PET and PEN homopolymers respectively. A maximum of 17.8 nm is reached at the 60% PEN composition. These results are similar to that found in PET/PEN copolymers [44], in which Lu and Windle found that the long period reached a maximum at intermediate PEN concentrations. Also shown in Fig. 13 are the values of l_1 and l_2. The value of l_1 increases slightly with increasing PEN content, but remains relatively constant when compared to L or l_2. On the other hand, the value of l_2 varies nearly proportionally to the long period as a function of composition. Since WAXS indicated the minor component was being trapped in the amorphous phase and l_1 is more typical of the size for the crystallite dimensions, it is concluded that l_1 is the crystallite dimension and l_2 the interlamellar amorphous dimension.

It is seen that the interlamellar amorphous height increases greatly as the composition of the minor component increases. Furthermore, the PEN, as a minor component, has less effect on the amorphous region of the PET rich blends compared to the effect of PET on the PEN rich blends. This is shown from the amorphous phase increases, which are faster for the PEN rich blends in comparison to the PET rich blends. Finally, adding of a small amount of the minor component significantly increases the height of the interlamellar amorphous region, as shown by the 5% PEN blend.

These results complete the overall picture of the structures and morphologies of the blends when crystallized quiescently. From WAXS, it is shown that the blends crystallize independently with the minor component being forced into the amorphous region. The crystalline structure is the same crystalline structure as that of the major component. The dominant morphology is interlamellar, such that the interlamellar amorphous height increases as the composition of the minor components increases. As a result, the long period also increases as the percentage of the minor component increases.

4.4. Density

Fig. 14 shows the densities of the blends as a function of temperature for various compositions. As is seen, the densities decrease with increasing PEN composition. This is linked to the fact that the crystalline and amorphous densities of PEN are lower than those of PET. Fig. 14 also shows that the densities of all compositions, except that of the 40% PEN blend, increase with increasing crystallization temperature, due to the increased crystal perfection. For the 40% PEN blend, the curve increases initially, decreases and then levels off with increased crystallization temperature.

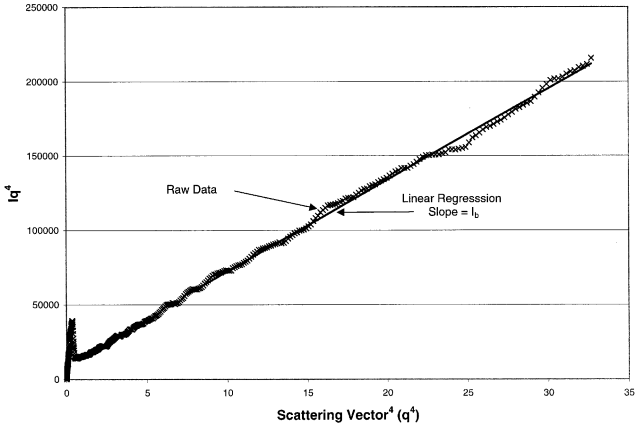

Fig. 10. Determination of Porod constants.

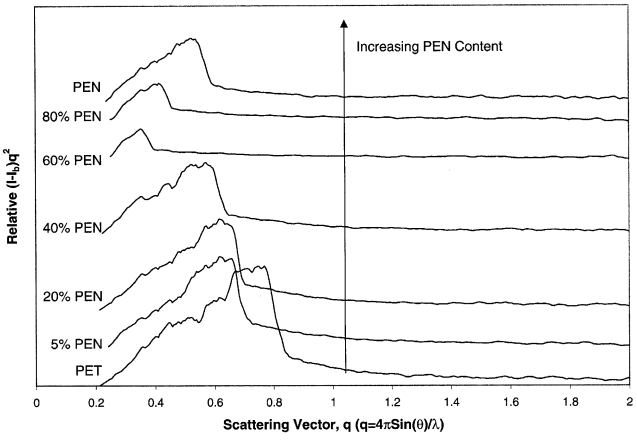

Fig. 11. Desmeared SAXS profiles for various PET/PEN blends and homopolymers.

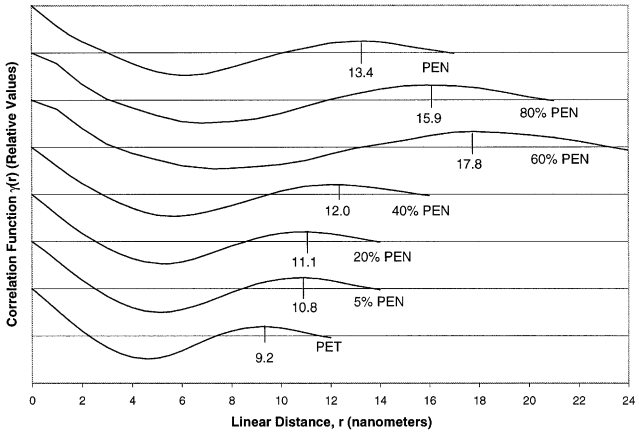

Fig. 12. Correlation functions for quiescently crystallized PET/PEN samples.

This was not expected since PET and PEN crystallize to greater extents as the degree of supercooling decreases. The explanation for this phenomena is linked to the WAXS results for the blend shown in Fig. 2. At low crystallization temperatures, only PET was found to be crystallizing. As the temperature increased, both PET and PEN crystallized. At intermediate crystallization temperatures, the PEN is likely interrupting the PET from crystallizing to its full extent. As a result, the density decreases slightly before becoming constant with increasing crystallization temperature.

To calculate the weight percent crystallinity (M_c), Eq. (8) was used

$$M_c = 100(\rho_{\text{crystalline phase}}/\rho_{\text{sample}})[(\rho_{\text{sample}} - \rho_{\text{amorphous phase}})/(\rho_{\text{crystalline phase}} - \rho_{\text{amorphous phase}})] \quad (8)$$

The compositional makeup of the amorphous and crystalline phases are unknown; therefore, some assumptions have been made. WAXS shows that only PET has crystallized for

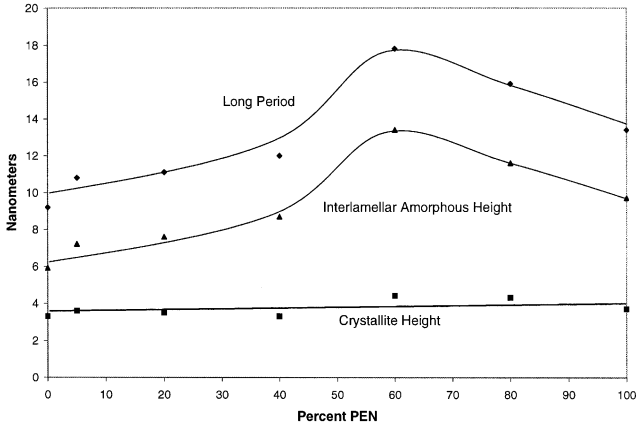

Fig. 13. Effect of blend composition on the long period, crystallite height, and interlamellar amorphous height, obtained with SAXS.

the 5 and 20% PEN blends. This means the amorphous phase consists of the PEN and the portion of PET that did not crystallize. For the 60 and 80% PEN blends, only PEN crystallized. For these samples, the amorphous phase contains PET and the uncrystallized portion of PEN. From this, it is assumed that each component of the blends would achieve the same level of crystallinity as that of the pure material. Therefore, if pure PET homopolymer crystallized to 65% normally, then a 20% PEN blend would exhibit a crystallinity of 52% if only the PET portion of the blend crystallized. Using this value and a basis of 100 mg, the relative ratios of amorphous and crystalline fractions were calculated as shown in the following example.

$$\text{Amorphous PEN} = 0.2 \times 100 = 20 \text{ mg} \quad (9)$$

$$\text{Amorphous PET} = (0.8 \times (1 - 0.65) \times 100 = 28 \text{ mg} \quad (10)$$

$$\text{Crystalline PET} = (0.8 \times 0.65) \times 100 = 52 \text{ mg} \quad (11)$$

$$\text{Total} = 100 \text{ mg}$$

Since volumes are additive, the following is true

$$V_{\text{am Sample}} = V_{\text{am PET}} + V_{\text{am PEN}} \quad (12)$$

$$m_{\text{am sample}}/\rho_{\text{am Sample}} = m_{\text{am PET}}/\rho_{\text{am PET}} + m_{\text{am PEN}}/\rho_{\text{am PEN}} \quad (13)$$

$$1/\rho_{\text{am Sample}} = m_{\text{am PET}}/(m_{\text{am sample}})(\rho_{\text{am PET}}) + m_{\text{am PEN}}/(m_{\text{am sample}})(\rho_{\text{am PEN}}) \quad (14)$$

where m is the Mass, V, the Volume, ρ, the Density and am is the Amorphous

In Eq. (14), mass of the amorphous PET divided by the mass of the amorphous sample is the fraction of amorphous content; therefore

$$1/\rho_{\text{am Sample}} = X_{\text{am PET}}/\rho_{\text{am PET}} + X_{\text{am PEN}}/\rho_{\text{am PEN}} \quad (15)$$

where $X_{\text{am PET}}$ is the fraction of Amorphous PET, $X_{\text{am PEN}}$ is the fraction of amorphous PEN.

This is the value used as the amorphous density in Eq. (8). For the amorphous densities of the pure material in Eq. (15), 1.333 g/cm^3 [58] and 1.325 g/cm^3 [60] were used for PET and PEN, respectively. For the crystalline density, 1.455 g/cm^3 [33] was used for the PET crystallizing blends and 1.407 g/cm^3 for the PEN crystallizing blends. For the 40% PEN blends and the SIC blends, the crystalline densities for both components were calculated in a manner analogous to that of the amorphous density as just described, since both PET and PEN are found in the crystalline and amorphous phases.

The resulting crystallinities are shown in Fig. 15. Along with these, are the samples that were strain induced crystallized and annealed. The latter are plotted at their annealing temperatures. It has been previously found that annealed strain induced crystallized samples should achieve the

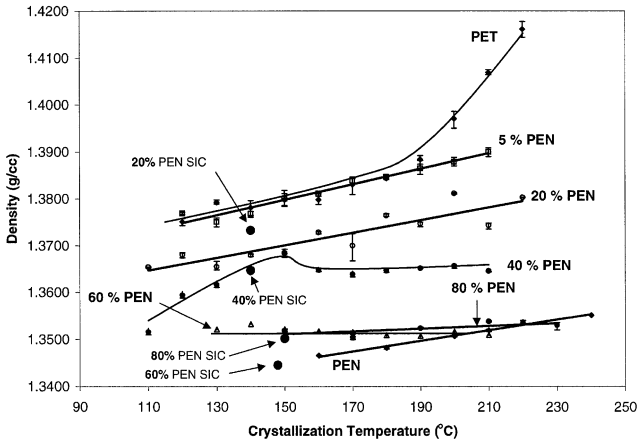

Fig. 14. Densities of blends quiescently crystallized from 110–240°C as well as for blends strain induced crystallized and then annealed from 140–150°C.

same level of crystallinity as those of quiescently crystallized samples [58]. This however may or may not be true for the blends since the type of crystallization results in different crystal systems. Strain induced crystallization results in a mixed crystal system, in which both PET and PEN crystallize. Quiescent crystallization results in independent crystallization, in which only the major component of the blend crystallizes. Therefore, it is conceivable that strain induced crystallized blends could crystallize to a further extent since there is more crystallizable material present in these blends. This may be why the 20% PEN strain induced crystallized sample exhibits a higher density than the 20% PEN quiescently crystallized sample. Currently, this is under further investigation.

5. Conclusion

Melt blending of PET and PEN creates copolymers through transesterification. These copolymers differ from those prepared through direct synthesis such that the nature of the resulting material is dependent not only on the composition of the blend, but also on the extent of transesterification. The structures and morphologies of the blends are; therefore, also highly dependent on the extent of transesterification. At reaction levels lower than the critical extent of transesterification, WAXS analysis of quiescently crystallized blends shows that the PET and PEN components crystallize independently of one another into separate phases. For blends surpassing their critical extent of transesterification, the natures of these blends are dependent only on their composition, and not on the extent of transesterification. Furthermore, the crystal structures and morphologies are controlled by the mode of crystallization. Quiescent crystallization leads to independent crystallization of the major component with the minor component being rejected into the amorphous phase. In strain induced crystallization of the blends, the nature of the structures is such that both PET and PEN co-crystallized together in the crystalline regions. The differences created by the two modes of crystallization are attributed to their crystallization kinetics, since strain induce crystallization is a very rapid process as compared to quiescent crystallization.

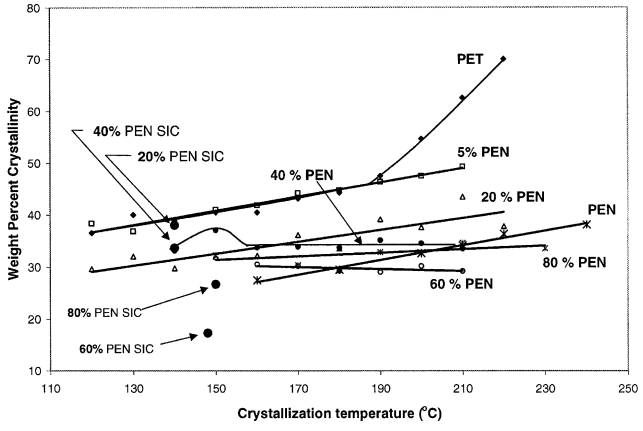

Fig. 15. Percent crystallinities of blends quiescently crystallized from 110–240°C as well as for blends strain induced crystallized and then annealed from 140–150°C.

Acknowledgements

We would like to thank the members of the PET consortium who support our research at the Polymer Institute, University of Toledo.

References

[1] McGee TM, Jones AS. Effect of processing parameters on physical properties of PET/PEN blends for bottle applications. In: SPE 11th Annual High Performance Blow Molding Conference 1996. p. 91–106.
[2] Jones AS, Dickson TJ, Wilson BE. Polymer preprints ACS Mar 1996:229–30.
[3] Aoki Y, Li L, Amari T, Nishimura K, Arashiro Y. Macromolecules 1999;32:1923–9.
[4] Bauer CW. Antec 1997:1578-81.
[5] McDowell CC, Freeman BD, McNeely GW, Haider MI, Hill AJ. J Polym Sci 1998;36:2981–3000.
[6] Ahmada O, Ezquerra TA, Nogales A, Balta-Calleja FJ, Zachmann HG. Macromolecules 1996;29:5002–9.
[7] Po R, Occhiello E, Giannotta G, Pelosini L, Abis L. Polym Adv Technol 1996;7:365–73.
[8] Kit KM, Schultz JM, Gohil RM. Polym Engng Sci 1995;35(8):680–92.
[9] Wu G, Cuculo JA. Polymer 1999;40:1011–8.
[10] Cakmak M, Wang YD, Simhambhatla M. Polym Engng Sci 1990;30:721–33.
[11] Aoki Y, Li L, Amari T, Nishimura K, Arashiro Y. Macromolecules 1999;32:1923–9.
[12] Shi Y, Jabarin SA. Glass transition and melting behavior of poly(ethylene terephthalate)/poly(ethylene 2,6-naphthalate blends. J Appl Polym Sci 2001;81:11–22.
[13] Kotliar AM. J Polym Sci, Macromol Rev 1981;16:367–95.
[14] Kimura M, Porter RS. J Polym Sci, Polym Phys Ed 1983;21:367–78.

[15] Okamoto M, Kotaka T. Polymer 1997;38(6):1357–61.
[16] Porter RS, Jonza J, Kimura M, Desper C, George E. Polym Engng Sci 1989;29(1):55–62.
[17] Andresen E, Zachmann HG. Colloid Polym Sci 1994;272:1352–62.
[18] Kim JC, Cakmak M, Geil PH. Antec 1997:1572–7.
[19] Stewart M, Cox AJ, Naylor DM. Polymer 1993;34(19):4060–7.
[20] Shi Y, Jabarin SA. Transesterification reaction kinetics of poly(ethylene terephthalate)/poly(ethylene 2,6-naphthalate) blends. J Appl Polym Sci 2001;80:2422–36.
[21] Kenwright AM, Peace SK, Richards RW, Bunn A, Macdonald WA. Polymer 1999;40:5851–6.
[22] Yamadera R, Murano M. J Polym Sci 1967;5(A-1):2259–68.
[24] Devaux J, Godard P, Mercier JP. J Polym Sci, Polym Phys Ed 1982;20:1875–80.
[25] Devaux J, Godard P, Mercier JP. J Polym Sci, Polym Phys Ed 1982;20:1881–94.
[26] Devaux J, Godard P, Mercier JP. J Polym Sci, Polym Phys Ed 1982;20:1895–900.
[27] Devaux J, Godard P, Mercier JP. J Polym Sci, Polym Phys Ed 1982;20:1901–7.
[28] Kenwright AM, Peace SK, Richards RW, Bunn A, Macdonald WA. Polymer 1999;40:5851–6.
[29] Lee SC, Yoon KH, Park H, Kim HC, Son TW. Polymer 1997;38:4831–5.
[30] Y Shi. PhD Thesis. Study on PET/PEN blends: transesterification reaction and properties, University of Toledo, Advisor Dr S. Jabarin, 1997.
[31] Tharmapuram SR, Jabarin SA. Antec 2000:1761–4.
[32] Tharmapuram SR, Jabarin SA. Antec 2000:2120–4.
[33] Daubeny RP, Bunn CW, Brown CJ. Proc R Soc 1954;226A:531–42.
[34] Fakirov S, Fisher EW, Schmidt GF. Makromol Chem 1975;176:2459–65.
[35] Kinoshita Y, Nakamura R, Kitano Y, Ashida T. Polym Prepr 1979;20:454.
[36] Buchner S, Wiswe D, Zachmann HG. Polymer 1989;30:480–8.
[37] Liu J, Myers J, Geil PH, Kim JC, Cakmak M. Antec'97 1997:1562–6.
[38] Mencik Z. Chemicky Prumysl 1967:78–81.
[39] Cakmak M, Kim JC. Antec'97 1997:1616–20.
[40] Shi Y, Jabarin SA. Crystallization kinetics of poly(ethylene terephthalate)/poly(ethylene 2,6-naphthlate) blends. J Appl Polym Sci 2001;81:23–37.
[41] Flory PJ. J Chem Phys 1958;29:1395.
[42] Wunderlich B. J Chem Phys 1958;29:1395.
[43] Windle AH, Viney C, Golombok R, Donald AM, Mitchell GR. Faraday Discuss Chem Soc 1985;79:55.
[44] Lu X, Windle AH. Polymer 1996;37(11):2027–38.
[45] Lu X, Windle AH. Polymer 1995;36(3):451–8.
[46] Jun HW, Chae SH, Park SS, Myung HS, Im SS. Polymer 1999;40:1473–80.
[47] Park SS, Chae SH, Im SS. J Polym Sci, Part A: Polym Chem 1998;36:147–56.
[48] Wu G, Cuculo J. Polymer 1999;40:1011–8.
[49] Souffer, et al. US Patent 571 262 February 3, 1998.
[50] Chung FW, Scott RW. J Appl Crystallogr 1973;6:225–30.
[51] Alexander L. X-ray diffraction methods in polymer science. New York, 1969.
[52] Hsiao BS, Sauer BB. J Polym Sci, Part B: Polym Phys 1993;31:901–15.
[53] Strobl GR, Schneider M. J Polym Sci, Polym Phys Ed 1980;18:1343–59.
[54] Strobl GR, Schneider M, Voigt-Martin IG. J Polym Sci, Polym Phys Ed 1980;18:1361–81.
[55] Cruz CS, Stribeck N, Zachmann HG. Macromolecules 1991;24:5980–90.
[56] Verma RK, Velikov V, Kander RG, Marand H, Chu B, Hsiao BS. Polymer 1996;37(24):5357–65.
[57] Bragg WL. Proc Cambridge Phil Soc 1913;17:43–57.
[58] Fischer EW, Fakirov SJ. J Mater Sci 1976;11:1041.
[60] Ghanem AM, Porter RS. J Polym Sci 1989;27:2587–603.